Evaluating seal capacity of caprocks and intraformational barriers for the geosequestration of CO_2

R. F. Daniel[1, 2] and J. G. Kaldi[1, 2]

Abstract

The petrophysical properties of cap rocks and intraformational barriers can constrain the carbon dioxide (CO_2) containment volumes of potential geosequestration sites. Characterisation of regional seals and intraformational barriers requires an understanding of the seal capacity of the cap rock or barrier. Seal capacity is the capillary pressure (or column height) at which a trapped fluid commences to leak through a seal rock. Seal rocks are effective due to very fine pore and pore-throat sizes that result in low porosities and permeabilities. These in turn generate high capillary threshold pressures. High threshold pressures, together with wettability and interfacial tension (IFT) properties determine the final column height that a seal can hold. Wettability and IFT play an important role in the geological storage of CO_2 through their effect on seal capacity (CO_2 column height) with respect to capillary pressure, thereby controlling the potential for the movement of CO_2 through the seal and affecting ultimate reservoir storage volumes.

Mercury injection capillary pressure analysis has been used extensively in the petroleum industry to determine the effectiveness of the top seal in relation to hydrocarbon column height retention. With the burgeoning interest in geological storage of CO_2, this technology can be applied to establish the suitability of a top seal for containment of CO_2; however, the role of IFT and wettability in the CO_2-water-rock systems is not well understood. It is unclear how supercritical CO_2 ($scCO_2$) affects these two properties, particularly as the water front becomes saturated with $scCO_2$ and eventually becomes miscible with the $scCO_2$ at high pressure reservoir conditions.

Selected examples of top and intraformational seals from the Bowen, Otway, Gippsland and Cooper basins are discussed in light of new experimental evidence on wettability and IFT variations in the CO_2-water-rock system. These variations may be more significant than in hydrocarbon-water-rock systems and based on non-wetting assumptions, the calculated CO_2 column heights may be significantly different than previously predicted.

Keywords: geosequestration, carbon dioxide, CO_2, seal capacity, wettability, reservoir.

Introduction

The evaluation of regional and local top seals has been a significant component in petroleum exploration. Seal evaluation is also being utilised in the new realm of CO_2 geological storage, in order to determine whether a confining seal will support an injected volume of CO_2 for a significant period of time.

Seal capacity or column height determination, using mercury injection capillary pressure (MICP) analysis, has been utilised in the petroleum industry since the technique was developed by Purcell (1949) and refined by Picknell et al. (1966) and Wardlaw and Taylor (1976). The background theory to MICP analysis is presented in the methodology section. The methodology also demonstrates the importance of the wettability and interfacial tension (IFT) parameters in determining column height in the analytical procedure.

The sealing capacity of a rock is a function of pore-throat size, contact angle (wettability) and interfacial tension. The column height of hydrocarbon or CO_2 in a reservoir therefore increases as (a) pore throat size in the seal decreases; (b) the contact angle (wettability) between hydrocarbon or CO_2 -water -rock decreases and (c) the interfacial tension between hydrocarbon or CO_2 and water increases (Fig. 1).

The minerals present in seal and reservoir rocks are generally assumed to be water wet, however research investigating reservoir production problems suggest that reservoir and seal rocks can range between water-wet (miscible phase) and oil-wet (immiscible phase) (Robin 2001; Benson and Cook 2005). Wettability can be evaluated by several methods. The most common method is the 'pendant drop' technique which is based on contact angle measurements of the immiscible phase (oil or CO_2) placed on a mineral surface in the presence of the miscible phase (water). In order to determine CO_2 column height using MICP analysis, it is necessary to know the contact angle and interfacial tension of the CO_2-water-rock system, so that the mercury/air pressure system can be converted to an equivalent CO_2/water pressure system. The contact angle and IFT can be measured at subsurface pressure/temperature (P/T) conditions by viewing through windows in high pressure cells constructed for this purpose.

Two other analytical methods commonly used by oil industry and service companies are the United States Bureau of Mines (USBM) and Amott/IFP methods. These methods give a numerical indication or index of wettability, rather than a contact angle (see Anderson 1986 and Robin 2001). It is not possible to use the USBM/Amott methods on very fine grained rocks, as found in typical seals because of the rapid dispersal of clay minerals and the difficulty of integrating these results into the mercury/air to CO_2/water conversion calculations.

Important considerations are the phase properties of CO_2 and formation water, once the water acidifies from CO_2 dissolution. These factors tend to alter the wettability up to and into the supercritical P/T range. Once the supercritical P/T has been reached the CO_2 and water becomes fully miscible and therefore fully wetting without interfacial tension between the two fluids.

1. Cooperative Research Centre for Greenhouse Gas Technologies (CO2CRC),
2. Australian School of Petroleum, The University of Adelaide, Adelaide, SA 5005, Australia
rdaniel@asp.adelaide.edu.au

This area of research contains very little experimental evidence on a) the state of the CO_2 charged water and, b) its effect on seal rock mineralogy with respect to capillary pressure. These are pertinent to the associated controls in determining CO_2 column height of the sealing lithology (Yang and Gu 2004; Yang et al. 2005).

Methodology

Mercury Injection Capillary Pressure

Mercury injection capillary pressure (MICP) analysis is based on a technique which is rate-limited, as predicted by the Darcy equation. This equation describes the general function of flowrate vs. pressure drop:

$$V = \frac{1}{\alpha}\frac{g_c}{\mu}\frac{\Delta\rho}{L} \qquad (1)$$

Where V is the superficial velocity of fluid, 1/α is the permeability coefficient, g_c is a dimensional gravity constant μ is the fluid viscosity, Δρ is the pressure differential and L is the pore length. The velocity of flow in a viscous liquid, such as mercury, is proportional to the pressure drop and inversely proportional to the length and surface area of the pore. Hence, given a specific limited flow velocity, the complete filling of a porous network will be a function of time. The larger the volume of pores the more time required to fill the total pore volume. Therefore, mercury porosimetry is most accurate when mercury is given sufficient time to fill all the available pores at the same pressure (equilibration).

Pore Throat Size Determination

MICP analysis uses the physical principle that a non-reactive, non-wetting liquid will only penetrate a porous medium once sufficient pressure is applied to force its entrance into the pore system. The relationship between the applied pressure and the pore throat radius into which mercury will intrude is given by the modified Washburn (1921) equation, as suggested by Purcell (1949) and Schowalter (1979):

$$P_c\, r = 2\,\sigma\cos\theta \qquad (2)$$

Where P_c is the applied capillary pressure, r is the pore throat radius, σ is the surface tension of mercury (481 mN/m) and θ is the contact angle between mercury and the pore wall (usually 140º) (Fig 1).

These equations assume that all pores are right circular cylinders. As pressure increases during analysis, the MICP instrument senses the intrusion volume of mercury by the change in capacitance between the mercury column and a metal sheath surrounding the stem of the penetrometer (Vavra et al. 1992a and b). The pressure and volume data are continuously acquired by an attached computer as the mercury column shortens in the stem and intrudes the sample.

The following values for the air-mercury system can be used to convert this capillary pressure data to effective pore throat size (Vavra et al 1992a & b):

- Air/mercury contact angle ($\theta_{a/m}$) = 140º;

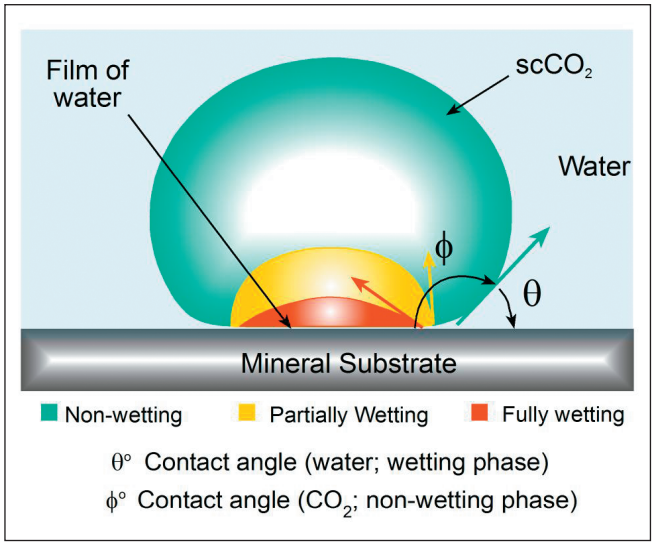

Figure 1. Cartoon of a droplet of $scCO_2$ (green) on a mineral substrate. The contact angle of the wetting phase (θ) is measured through the non-wetting phase (φ) i.e. θ = 180º – φ. The continuum to fully wetting is shown in the yellow and red droplets *modified from* Chiquet and Broseta (2005).

- Interfacial tension ($\theta_{a/m}$) = 481 mN/m;
- ($\theta_{a/m}$)*cos($\theta_{a/m}$) ≈ 368

These result in the following relationship of capillary pressure to pore throat radius:

1 psi ≈ 100 µm; 10 psi ≈ 10 µm; 100 psi ≈ 1 µm; 1000 psi ≈ 0.1 µm

Determination of Seal Capacity or Column Height

MICP analytical data is also used to determine the maximum column height and the water saturation of the sedimentary rock as a function of height above the free water level (FWL). This data must be converted to a subsurface CO_2/water system before the mercury injection data can be used to determine seal capacity (column height). The following equation can be used (after Schowalter 1979):

$$P_{bCO_2} = P_{a/m}\frac{\left(\sigma_{b/CO_2}\cos\theta_{b/CO_2}\right)}{\left(\sigma_{a/m}\cos\theta_{a/m}\right)} \qquad (3)$$

Where P_{b/CO_2} is the capillary pressure in the water/CO_2 system, $P_{a/m}$ is the capillary pressure in the air/mercury system, σ_{b/CO_2} and $\sigma_{a/m}$ are the interfacial tensions of the water/CO_2 and the air mercury systems respectively, θ_{b/CO_2} and $\theta_{a/m}$ are the contact angles of the water/CO_2/substrate and air/mercury/substrate systems respectively.

As highlighted in equation (3), the role of wettability (contact angle) and interfacial tension (IFT) in determining column height is significant. In the petroleum industry these parameters are known experimentally through extensive research using synthetic and proxy hydrocarbons, which agree with subsurface conditions as demonstrated by Smith (1966); Schowalter (1979); Anderson (1986); Zhang et al. (1997); Bi et al. (1999); Al-Siyabi et al. (1999) and Morrow (1990). In the geological storage of carbon dioxide, the role of wettability is not well known with little published

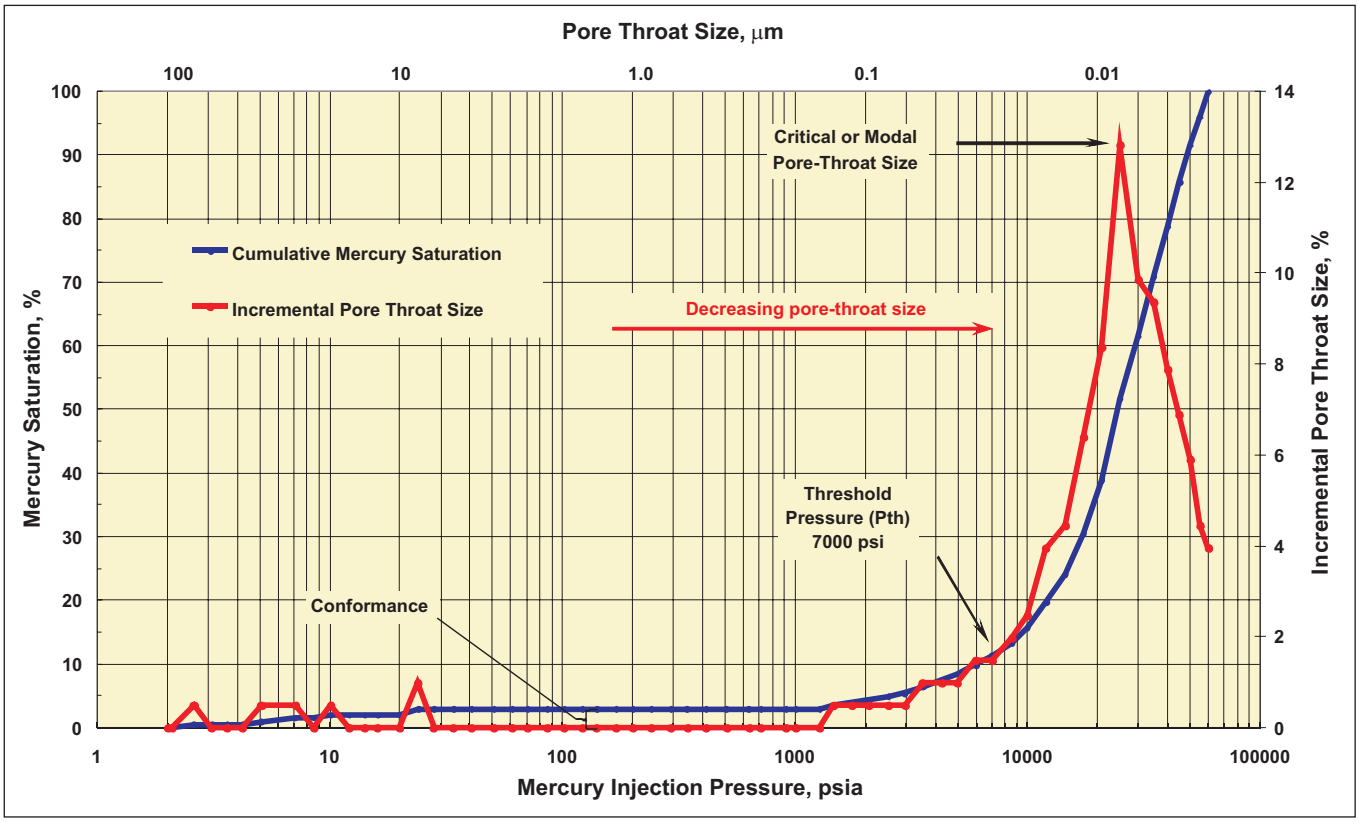

Figure 2. Mercury injection capillary pressure analysis nomenclature: Conformance; pressure/volume increment due to surface rugosity: Threshold pressure (Pth); commencing to form a continuous mercury filament through the rock.

research available (Yang and Gu 2004; Hildenbrand et al. 2004; Chiquet et al. 2007; Chalbaud et al. 2006; Bennion and Bachu 2006).

Buoyancy pressure drives CO_2 (non-wetting phase) movement in the subsurface and forces it into the pore throats of a rock, subsequently displacing water (wetting phase). Buoyancy is the density difference (g/cc) between CO_2 and water multiplied by the column height (ft) and the pressure gradient of water due gravity (0.433 psi/ft). In other words, the greater the column thickness of CO_2, the greater the buoyancy pressure forcing CO_2 into the pore network. Threshold pressure (Pth) is the pressure at which the non-wetting phase (mercury or CO_2) begins to flow through the rock as a continuous phase (Fig. 2). This pressure is determined graphically by, (a) combining the injection and incremental pore-throat size curves, (b) determining the point at which the pore-throat size distribution curve approaches the critical pore-throat size (modal pore-throat size), and (c) the point at which the injection curve has its maximum inflection upwards, as described by Kivior et al. (2002) and refined by Dewhurst et al. (2002) (Fig. 2).

A CO_2 geosequestration reservoir is made up of rocks with different pore throat sizes. These pore throats will have different displacement and threshold pressures, and varying CO_2 saturations as a function of height (h) above the free water level or maximum storage height (FWL). In any given CO_2 charged reservoir, the lowest indication (or maximum height) of CO_2 in a particular rock type approximates the threshold pressure (Pth) for that rock. The Pth (equivalent column height) can thus be considered as the CO_2/water contact for that particular rock type. It should be noted that a reservoir with multiple rock types may have several corresponding CO_2/water contacts, but will have only one FWL. It is therefore of significance to determine the FWL, which is required to ascertain the maximum column height (h_{max}) of CO_2 (or any non-wetting fluid) in the reservoir (Schowalter 1979).

In order to determine h_{max}, capillary pressure data must first be converted to height above free water level by using the equation:

$$Pc_{b/CO_2} = h\ (\rho b\text{-}\rho co_2)\ 0.433 \qquad (4)$$

Then H_{max} is calculated using Equation 5 (Smith 1966; Vavra et al. 1992a)

$$h_{max} = (Pth_s - Pth_r) \div (\rho b\text{-}\rho co_2)\ 0.433 \qquad (5)$$

Where Pc_{b/CO_2} is the capillary pressure (psi) reservoir water/CO_2 system, h is the height (in ft), ρb is the subsurface water density (g/cc), ρ_{CO_2} is the subsurface CO_2 density (g/cc), Pth_s is the threshold (displacement) pressure of the seal and Pth_r the threshold (displacement) pressure of the reservoir.

Typical Australian subsurface properties for supercritical CO_2 are variable, with density ranging from 0.42–0.74 g/cc and water density ranging from 0.97 to 1.05 g/cc for brines ~5000 to ~65000 ppm, although higher salinities (with commensurate densities) are known from some formations (from converted field data using Rowe and Chou (1970) and Span and Wagner (1996)).

Interfacial tension, CO_2 and water densities are determined using calculations after Span and Wagner (1996) and Rowe and Chou (1970). Generally the interfacial tension for water/CO_2 varies from 21 to 27 mN/m and the contact angle is usually assumed to be 0º (wetting phase). Once the capillary pressure values have been converted to h (height, ft or converted metres), height versus mercury (non-wetting phase) saturations can be plotted. Conversion of mercury (non-wetting phase) to CO_2 (non-wetting phase) yields a height versus CO_2 saturation plot. The non-wetting phase saturation can be converted to the water (wetting-phase)

saturation (Schowalter 1979), using the conversion:

$$S_w = 1 - S_{nw} \quad (6)$$

Where: S_w = wetting phase (water) saturation;

S_{nw} = non-wetting phase ($scCO_2$) saturation.

Using the Equations (5) and (6), a plot of column height (above FWL) with sensitivities versus water saturation can be graphed to estimate potential CO_2 storage volume at various water saturations.

Discussion

CO_2 leakage can take place through three main processes; 1) diffusion through the wetting phase, 2) capillary movement through the pore structure, and 3) migration through possible fracture networks. Zweigel et al. (2004) illustrated that capillary leakage starts at break-through pressure (threshold pressure) and stops when the pressure is reduced to around 20 -50% of the threshold pressure. However, the underlying assumption on these processes is that CO_2 is the non-wetting phase at sub-surface conditions. The following discussion examines this assumption in the light of recent experimental evidence.

CO_2 Contact Angle

Until recently gas in the sub-surface, either hydrocarbon gas or CO_2/water/rock was assumed to have a contact angle (θ) of 0º, as water was thought to be the wetting phase (Schowalter 1979). Experimental work by Morrow et al. (1973) to determine wettability factor used the general assumption that most rocks are preferentially water wet, which can be expressed as;

$$Wettability = \sigma_{b/CO_2} .cos\ \theta_{b/CO_2}$$

Where σ is the interfacial tension and θ is the contact angle of CO_2/water/rock.

Pore-level injection modelling, incorporating a distribution of varying pore-throat radii and formation wettability (including contact angle, IFT and fluid viscosities) developed by Ferer et al. (2002), also assumed that the injected CO_2 was immiscible in a water wet porous medium (CA = 0º). However Bath (1989) found that miscibility occurs at relatively low pressures with CO_2 and recommended nitrogen for secondary and tertiary flooding as, unlike CO_2, nitrogen is only miscible at very high reservoir pressures.

Substrate / Salinity	Contact Angle (θ), Low Pressure < 0.5 MPa	Contact Angle (θ), High Pressure 10 MPa
Mica – 0.01M (584 ppm)	0º – 20º	60º – 80º
Mica – 0.1M (5820 ppm)	0º	40º – 60º
Mica – 1M (56000 ppm)	0º – 20º	60º – 80º
Quartz– 0.01M (584 ppm)	20º – 30º	40º – 55º
Quartz – 0.1M (5820 ppm)	0º – 10º	20º – 45º
Quartz – 1M (56000 ppm)	20º – 30º	40º – 55º

Table 1. CO_2/water/substrate contact angle (θ) variation with increasing salinity and pressure (*data* from Chiquet and Broseta, 2007).

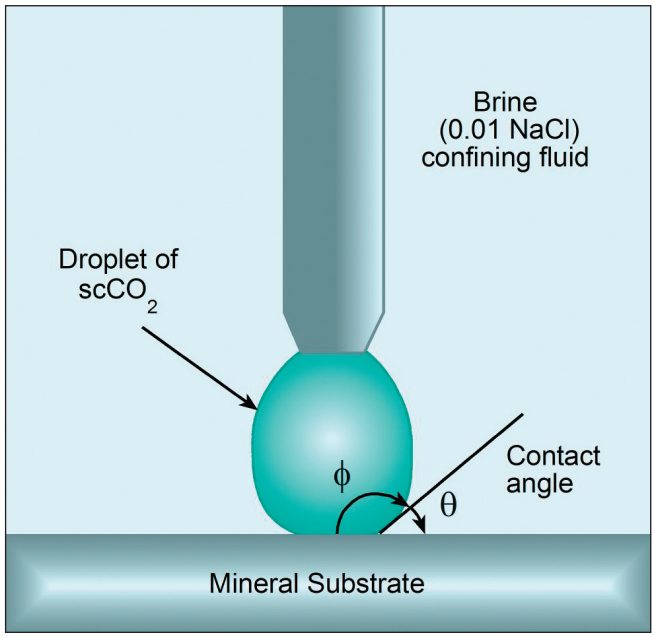

Figure 3. Cartoon of a droplet of $scCO_2$ being introduced onto a mineral substrate, at subsurface conditions, to determine the contact angle (after Chiquet and Broseta, 2005). Yang and Gu (2004) used a similar method, but introduced the water droplet via the needle into various CO_2 states to determine IFT at subsurface conditions.

CO_2 column heights were calculated for the Muderong Shale (a major top seal in the Carnarvon Basin, North West Shelf, Australia) by Dewhurst et al. (2002), who used the following data; interfacial tension of 25 mN/m, CO_2 density of 0.65 g/cm^3 and water density of 1.05 g/cm^3. A contact angle sensitivity analysis of between 0º and 45º was used, as there were little data available on $scCO_2$/water/rock contact angles at subsurface conditions. The maximum sensitivity resulted in a calculated reduction of CO_2 column height from 789 m to 558 m.

Recent experimental data by Chiquet and Broseta (2005), using $scCO_2$ droplets immersed in brine, showed that quartz and mica substrates (as proxy minerals for fine grained rocks) under low pressures (<1.0 MPa or 14.7 psi) become less water-wet in the presence of $scCO_2$, i.e. contact angles (θ) vary from 0º to 20º for mica (a clay proxy, having a similar structure to clay) and 20º to 30º for quartz. Under higher pressures (10 MPa or 1450 psi), the contact angle (θ) increases to 60º - 80º for mica and 40º - 55º for quartz (Table 1). The contact angles were measured through the CO_2 droplet (φ, see Fig. 1) and subtracted from 180º to give the wetting phase contact angle (θ). These experiments were carried out above the substrate in a pressure cell (Fig. 3). In a second part of the experiment, the CO_2 droplet was introduced beneath the mineral substrates in the pressure cell and the experiment repeated. The results were determined to be 10-15º less at low pressure with negligible differences at high pressures (Fig. 3). The purpose of the experiment below the substrate was to test the contact angle results against a buoyancy effect (Chiquet and Broseta 2005). Chiquet et al. (2007) also demonstrated that the difference in storage capacity between CO_2 as a non-wetting and

Non-wetting Phase	Depth of sample (m TVDSS)	Pressure at sample depth (MPa)	Temp at sample depth (ºC)	Salinity at sample depth	Non-wetting Phase Density (g/cm^3)	Water density (wetting phase) (g/cm^3)	Interfacial tension (mN/m or dynes/cm)	Contact Angle (º)	Seal Threshold Pressure (air-Hg system) (psia)	Seal Threshold Pressure (brine-CO_2 system) (psia)	Height of CO_2 Column (m)
OIL	1900	19	70	CO_2 Unsat	0.75	0.9861	22	10	6990	412	1226
OIL	1900	19	70	CO_2 Sat	0.75	0.9981	22	10	6990	412	1167
Methane	1900	19	70	CO_2 Unsat	0.2	0.9861	52	0	6990	989	884
Methane	1900	19	70	CO_2 Sat	0.2	0.9981	52	0	6990	989	871
CO_2	1900	19	70	CO_2 Unsat	0.6373	0.9861	26.6	0	6990	506	1019
CO_2	1900	19	70	CO_2 Sat	0.6373	0.9981	26.6	0	6990	506	985
CO_2 dissolution is 52 kg/1000 kg brine at the above pressure and temperature											

Table 2. Change in column height of subsurface fluids from the effect of CO_2 saturation resulting in higher water density.

as a partially wetting phase (CA - 74º) would be approximately 69% less at 1200 m as a result of the commensurate lowering of the capillary membrane seal pressure (i.e. a reduced column height) due the changes in wettability.

The contact angle (CO_2-water- mica or quartz) is also affected by brine concentrations. For instance, θ decreased by ~20º from 0.01 M NaCl to 0.1 M NaCl then increased by ~20º from 0.1 M NaCl to 1 M NaCl brine solutions (Table 1). A decrease in CO_2 solubility also occurred with increasing salinity (Chiquet and Broseta 2005; Chiquet et al. 2007). These experiments were carried out on single mineral plates rather than a shale rock surface. Experimental scCO_2/water/rock contact angle studies on shale surfaces have not been reported in the literature.

Wettability determinations by Yang et al. (2008) have also shown that the contact angle advances under the influence of high pressure. Experimental research, using the Vuggy Limestone (reservoir) rock at the Weyburn CO_2 storage site in Canada, illustrated that the contact angle advanced from 91.23º at 27ºC and 0.1 MPa (14.5 psi) to 116º at 27ºC and 12.01 MPa (1742 psi) and 130º at 27ºC and 25 MPa (3626 psi). This changed the scCO_2/water/rock system to a hydrophobic system; i.e. the water became the non-wetting phase. At a higher temperature (58ºC) the angle only advanced to 100º, which was attributed to each phase (CO_2 and water) permeating the other (Yang et al. 2008).

CO_2 Interfacial Tension

The calculation of CO_2-water interfacial tension is a function of pressure, temperature and CO_2 density, and is based on research by Span and Wagner (1996) and Rowe and Chou (1970). The experimental data range from 0-140ºC with pressures up to 70 MPa (10152 psi) (Span and Wagner 1996; Rowe and Chou 1970). As CO_2 dissolution into the formation water occurs, the IFT increases slightly under experimental conditions. However, this has not been demonstrated in a CO_2-water system at reservoir conditions (J. Ennis-King pers comm.).

Recent experiments in interfacial interactions (Yang and Gu 2004; Yang et al. 2005) between water droplets immersed in scCO_2 using the pendant droplet method under reservoir conditions, have found several changes in the physical relationship (a variation of Fig. 3, but the pendant droplets are water). The primary change is a significant increase in the water droplet size (swelling due to CO_2 saturation) with increasing pressure in the presence of CO_2, to a point where the droplet detaches from the needle. This is thought to be due to the solubility of CO_2 in the water to a point where the density difference is only 0.25 g/cm^3 and detaches due to gravity. A second change occurs with increasing pressure, which follows on from a density convergence where the water and CO_2 become completely miscible at elevated pressures (T= 58ºC (136.4ºF) and 12.238 MPa (1775 psi)). This means that the IFT between CO_2 and water becomes zero as there is no interface between them at these pressure-temperature conditions. Consequently, as there is now only a single phase, it is, by definition, the wetting phase, although this was questioned by Chalbaud et al. (2006) where they

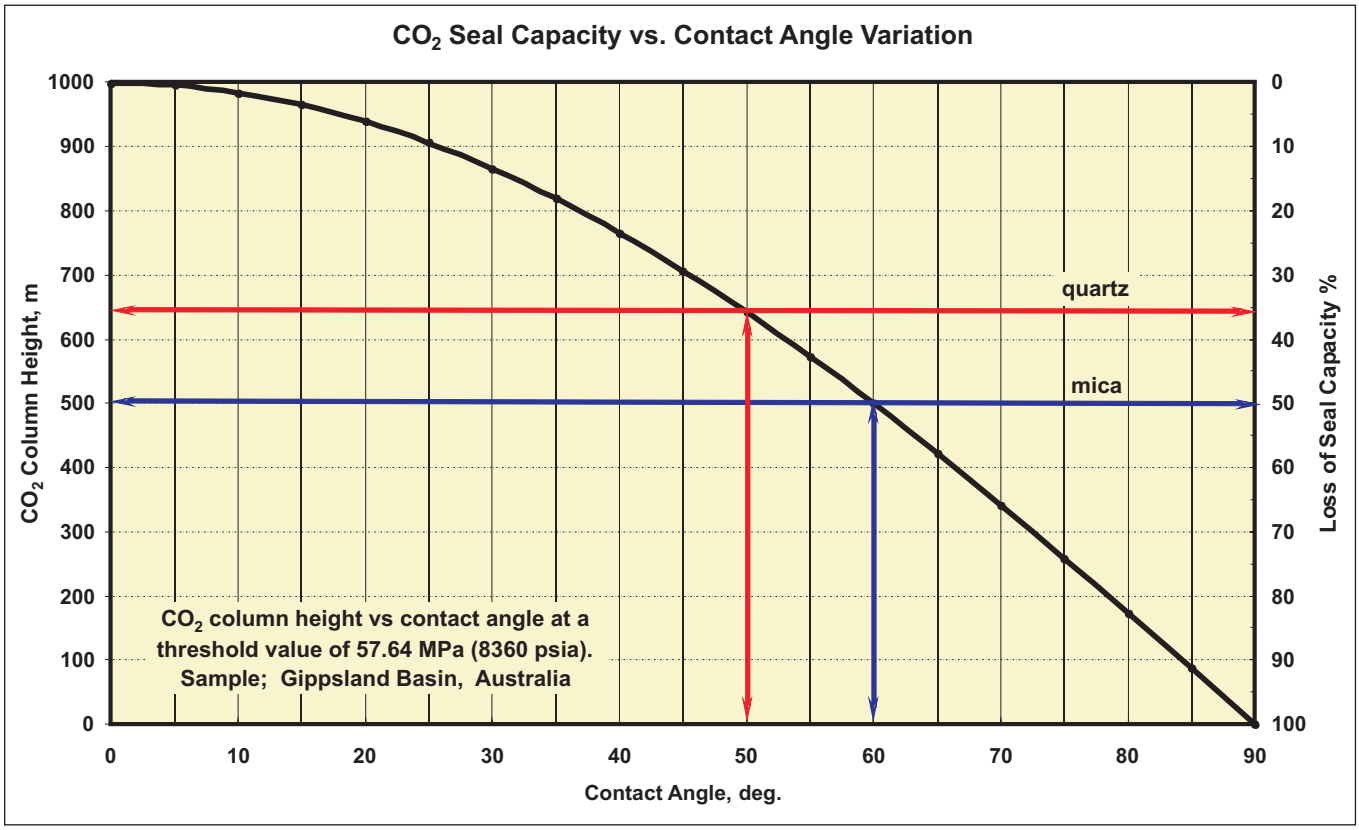

Figure 4. Graphic solution to increasing wettability (contact angle) versus column height of $scCO_2$ for quartz and mica substrates, based on equations (3) and (5).

experimentally determined water/CO_2 IFT's up to 25.5 MPa with varying salinities (5k, 50k, 100k and 150k ppm) and temperatures (27ºC, 71ºC and 100ºC). If an IFT of 0 mN/m is entered into the capillary equation (Equation 3) of Schowalter (1979) the resulting column height is zero. After this point it is assumed that the pore-throat size is the principle flow inhibitor through the seal.

Subsequently, Chiquet et al. (2006) performed pendant drop (water droplet in CO_2) experiments with temperatures from 34 to 109ºC (93 – 228ºF) and pressures from 5 to 45 MPa (725 – 6526 psi). The results generally showed that IFT was lowered with increasing pressure from 45.8 - 43.7 mN/m at 5 MPa with a temperature variation from 34 to 109ºC respectively, to 28.5 - 22.8 mN/m at 45 MPa with the same respective temperature variation. Both phases were saturated with respect to each other at the commencement of the experiments. Li et al. (2005) also found that the breakthrough pressure of CO_2 (IFT – 21 mN/m) was 38% of that for methane (IFT - 56.4 mN/m) and 33% of that for nitrogen (IFT - 57 mN/m). This demonstrated that the presence of CO_2 significantly changed the wettability of the Weyburn Midale Evaporite seal rock, indicating a requirement to re-evaluate potential seals once a site is selected for CO_2 storage (Li et al. 2005).

Effect of Dissolution on Seal Capacity

A study of the Miller Field (North Sea) found that natural CO_2 is dissolved in the reservoir fluids. Most of the CO_2 is present in the water phase (60-70 mol %) and the remainder in the oil phase (15-25%), which effectively increases the densities of both these phases (Baines and Worden 2000). In general, however, where depleted oil reservoirs or deep saline reservoirs are used for storage, the main form of trapping initially will be the dissolution of CO_2 into the formation water. The remainder will rise and be trapped beneath the cap rock seal and then migrate outwards to fill the trap. As more CO_2 dissolves into the water (aided by buoyancy pressure) it will become increasingly dense and set up a downward trending convection current, in turn also lowering the capillary pressure at the seal / reservoir interface. Over time, as CO_2 dissolution becomes complete, mineral trapping will occur depending on the mineralogy of the reservoir or seal rock (Ennis-King and Paterson 2001).

Reservoir simulations have shown that saturated CO_2 water becomes dense and sinks, countering the potential for top seal leakage of CO_2. An example of this phenomenon can be illustrated in Table 2, where the calculated differences in column heights are shown using fresh water and CO_2 saturated water. Despite an increase in water density due to CO_2 saturation, the parameters remain the same for each of the non-wetting phases highlighted in Table 2.

The solubility of CO_2 in water increases with increasing pressure, decreasing temperature and decreasing salinity. As a result, a significant amount of the trapped CO_2 dissolves in the formation water over time and complete saturation should occur over 10000s and 100000s of years depending on the reservoir permeability. Maximum solubility (~58 kg/1000 litres) occurs within a window around 20 MPa at 40ºC with <10,000 ppm salinity (after Ennis-King and Patterson 2003; Span and Wagner 1996; Rowe and Chou 1970).

Wettability and Carbonaceous Rocks

Research on the wettability effect of $scCO_2$ on coaly substrates suggests that the contact angle of CO_2-water-coal is considerably above 90º at subsurface conditions (>0.26 MPa). In other words, $scCO_2$ is fully wetting in the presence of coal

Formation	Depositional Environment	CO_2 Column Height (m) @CA 0º	CO_2 Column Height (m) @CA 20º	CO_2 Column Height (m) @CA 40º	CO_2 Column Height (m) @CA 60º
Bowen Basin		**Max / Min**	**Max / Min**	**Max / Min**	**Max / Min**
Snake Creek Mudstone	Marginal Marine	901 / 488	856 / 458	697 / 373	455 / 244
Formation	**Depositional Environment**	**CO_2 Column Height (m) @CA 0º**	**CO_2 Column Height (m) @CA 20º**	**CO_2 Column Height (m) @CA 40º**	**CO_2 Column Height (m) @CA 60º**
Otway Basin		**Max / Min**	**Max / Min**	**Max / Min**	**Max / Min**
Belfast Mudstone	Prodelta	850 / 607	799 / 571	651 / 465	419 / 356
Flaxmans Formation	Upper Deltaic Plain	987 / 713	928 / 670	756 / 546	494 / 356
Waarre Formation	Fluvial Overbank	1631 / 15	1533 / 14	1250 / 12	816 / 8
Formation	**Depositional Environment**	**CO_2 Column Height (m) @CA 0º**	**CO_2 Column Height (m) @CA 20º**	**CO_2 Column Height (m) @CA 40º**	**CO_2 Column Height (m) @CA 60º**
Cooper and Eromanga Basin		**Max / Min**	**Max / Min**	**Max / Min**	**Max / Min**
Murta Formation	Lacustrine	530 / 81	498 / 76	406 / 62	265 / 41
Birkhead Formation	Fluvio-Lacustrine	43 / 11	40 / 10	33 / 8	22 / 5
Cuddapan Formation	Flood Plain	834 / 90	784 / 84	639 / 69	417 / 45
Formation	**Depositional Environment**	**CO_2 Column Height (m) @CA 0º**	**CO_2 Column Height (m) @CA 20º**	**CO_2 Column Height (m) @CA 40º**	**CO_2 Column Height (m) @CA 60º**
Gippsland Basin		**Max / Min**	**Max / Min**	**Max / Min**	**Max / Min**
Latrobe Formation	Shelf	1070 / 17	1006 / 16	820 / 13	535 / 9
Gurnard Formation	Inner Shelf	723 / 41	680 / 38	554 / 31	362 / 20
Burong Formation	Back Barrier Lagoon	1191 / 63	1119 / 59	912 / 48	596 / 31
Kingfish Formation	Coastal Lake	764 / 53	718 / 50	585 / 41	382 / 26
Mackerel Formation	Shallow Marine	962 / 394	904 / 370	737 / 301	481 / 197
Note in all column height calculations P, T Salinity, densities, and IFT all constant for each sample					

Table 3. Examples of seal capacities from potential geological storage sites (Australia) and the effect of increasing wettability on column height (*data modified* from Daniel, 2005; Daniel and Kaldi, 2004; Gibson-Poole et al., 2006; and Sayers et al., 2006)

(from brown to black) and that anthracite is fully wetting at all pressures (Siemons et al. 2006). The implications of this are that coals cannot be expected to act as a capillary or membrane seal to CO_2. Similar conditions may apply to carbonaceous shales, accentuating the diffusion aspect of CO_2 transport (Siemons et al. 2006).

Experiments were conducted on ground coal (40 µm) particles to test the CO_2 adsorption qualities of water saturated coal under the influence of CO_2 injected at low pressure (37.5 kPa) in a confined test cell (Mazumder et al. 2003). At low pressures, water remained the wetting phase whilst the adsorption of CO_2 and desorption of CH_4 occurred at relatively

slow rates. Subsequently a high pressure cell was built. Results indicate that under higher injection pressures (~10 MPa) this exchange takes place at a faster rate, due to a change in wettability occurring as the CO_2 enters the wetting phase (Mazumder et al. 2003). This increases the movement and subsequent adsorption of CO_2 into the less water-wet coal with commensurate desorption of methane.

Seal Capacity Sensitivity Examples

The majority of the seals analysed by MICP analysis, using a contact angle of 0º, produced CO_2 column retention heights well above the thickness of the reservoir formations. However, as the sensitivity of increasing contact angle is applied (up to 60º), a reduction of the column height of up to 50% occurs (Fig. 4). Thus, seal potential of some rocks might be significantly lower than if assessed assuming a fully water-wet state (i.e. $\theta = 0º$). These rocks would no longer act as a membrane seal but might still act as a permeability baffle or an inhibitor to migration. Such baffling would increase residence time and thus increase the potential of dissolution and mineral trapping.

Rates of movement through fine grained muddy cap rock seal range from a minimum of 700 years per metre for $scCO_2$ (Lindeberg and Bergmo 2002) to 33,000+ years per metre for water (Dewhurst et al. 1999) for the low volumes that could migrate through these sub-micron pore throats. Dewhurst et al. (1999) shows a hydraulic conductivity data band from 10-16 to 10-10 m/s for water, which represents fluid migration rates from 3 µm to 30 mm/1000 years ($scCO_2$ when fully miscible with water may be similar). In studies of the Sleipner gas field (Norwegian North Sea), Lindeberg and Bergmo (2002) suggest that CO_2 will take more than 500,000 years to travel the 700 m to the sea floor at Sleipner via diffusion, and several million years to stabilise at very low ppm rates of leakage compared to the original injected volume. They also reiterate that CO_2 entry and pathway establishment through the seal is a function of the surface tension between the fluids (IFT) and the pore throat size distribution, so that ideally pore throat diameters would be <100 nm (nanometres).

These low rates of migration are not regarded as important leakage processes when considering long-term CO_2 storage, even at geological time scales. However, long residence time can lead to either a deterioration or enhancement of seal properties due to various diagenetic processes taking place during the CO_2 storage period (Hildenbrand et al. 2004). It is thus important to consider each potential site for possible local diagenetic reactions.

The CO2CRC (Australia) has identified several potential geological storage sites for CO_2, with the selection criteria based on sites having adequate reservoirs with significant confining top seals. These sites are located in the Gippsland, Otway (Victoria) and Bowen (Queensland) basins. The Cooper Eromanga Basin (South Australia) is included to increase the variety of depositional environments. Selected examples of sealing formations from these basins are presented to demonstrate the effect of increasing CO_2/water/rock contact angles on calculated column heights (Table 3). The available maximum and minimum column height variation from the formations are also shown to demonstrate that if the capacities of the seals are high enough, then they will still act as membrane seals at the highest contact angle sensitivity (i.e. 60º). It is only when the thickness of the reservoir formation or intended injection height is larger than the height of maximum sensitivity that leakage may become an issue. Table 3 also highlights the importance of careful sampling to ensure that an accurate estimate of the seal capacity is calculated, as cap rocks can have significant variations of lithology with commensurate variations of CO_2 column height retention.

Conclusions

In light of recent experimental data on wettability, it is recommended that, where there is no previous established history of hydrocarbon seal capacity associated with the reservoir in question, contact angle sensitivities ranging up to 60º are used in the calculation of CO_2 seal capacities (column heights).

If the capillary pressure of a seal was competent in supporting a column of hydrocarbon, then it is anticipated it would support a column (albeit smaller due to different fluid properties) of CO_2 at similar pressure and temperature and, if upward migration through the seal does occur, it would be at very slow rates. Reported rates of water movement through fine grained muddy cap rock seals are in the order of 3 µm – 30 mm/1000 years, with commensurate low leakage volumes. As an example, it is considered that CO_2 will take more than 500,000 years to reach the sea floor at Sleipner via diffusion, with a stabilised low ppm rate of leakage at several million years.

Experimental studies on shale surfaces have not been reported, however this study suggests that due to uncertainty, a range of contact angles should be used rather than a single value with emphasis on the lower column height for determining seal capacity. Similarly, organic rich shales will have limited potential as membrane seals to CO_2 containment, however have the potential to inhibit migration via baffling.

Acknowledgements

The authors wish to acknowledge the support of the Cooperative Research Centre for Greenhouse Technologies, Australia and fruitful discussions on CO_2 storage with fellow researchers, Catherine Gibson-Poole, Maxwell Watson and Jonathan Ennis-King from the CO2CRC research group. The manuscript was also enhanced by the constructive comments of Monique Warrington and Brad Field who reviewed this paper.

References

AL-SIYABI, Z., DANESH, A., TOHIDI, B., AND TODD, A. C., 1999. Variation of gas-oil-solid contact angle with interfacial tension: Petroleum Geoscience, v 5, p. 37-40.

ANDERSON, W., 1986. Wettability literature survey – Part 2; Wettability measurement: Journal of Petroleum Technology, November, 1986, SPE No. 13933, Society of Petroleum Technology, p 1246-1262.

BAINES, S. J., AND WORDEN, R. H., 2000. Geological disposal: Understanding the long term fate of CO_2 in naturally occurring accumulations: Proceedings of the Fifth International Conference on Greenhouse Gas Control Technologies (GHGT 5), p 311-316.

BATH, P. G. H., 1989. Status on miscible/immiscible gas flooding: Journal of Petroleum Science and Engineering, v. 2-3, p. 103-117.

BI, Z., ZHANG, Z., XU, F., QIAN, Y., AND YU, J., 1999, Wettability, oil recovery, and interfacial tension with an SBS-Dodecane-Kaolin System.: Journal of Colloid and Interface Science, v. 214, p. 368-372.

BENNION, D. B., AND BACHU, S., 2006, Dependence on temperature, pressure and salinity of the IFT and relative permeability displacement characteristics of CO_2 injected in deep saline aquifers; SPE No. 102138, 9p.

BENSON, S., AND COOK, P., (Coordinating lead authors), 2005, Underground Geological Storage (Chapter 5), in B. Metz, Davidson, O., de Coninck, H., Loos, M., and Meyer, L., ed., Carbon Dioxide Capture and Storage - Intergovernmental Panel on Climate Change: New York, Cambridge University Press, p. 197-276.

CHALBAUD, C., ROBIN, M., AND EGERMANN, P., 2006, Interfacial tension data and correlations of brine/CO_2 systems under reservoir conditions. SPE No. 102918, 11p.

CHIQUET, P., AND BROSETA, D., 2005, Capillary alteration of shaly caprocks by carbon dioxide. SPE No. 94183.

CHIQUET, P., BROSETA, D., AND THIBEAU, S., 2007, Wettability alteration of caprock minerals by carbon dioxide: Geofluids v. 7, p. 112-122.

CHIQUET, P., DARIDON, J-L., BROSETA, D., and THIBEAU, S., 2006. CO_2/water interfacial tensions under pressure and temperature conditions of CO_2 storage. Energy Conversion and Management, v.48, p. 736-744.

DANIEL, R.F., 2005, Boggy Creek Carbon Dioxide Seal Capacity Study, Otway Basin, Victoria, Australia. CO2CRC Publication No RPT05-0045, August 2005, 47p.

DANIEL, R. AND KALDI, J., 2004. Atlas of Australian and New Zealand Hydrocarbon Seals. Volume 3, APCRC Technical Workshop Proceedings, Program 1; Hydrocarbon Sealing Potential of Faults and Cap Rocks. Perth, WA, June 2004. 220p.

DEWHURST, D. N., JONES, R. M., AND RAVEN, M. D., 2002, Microstructural and petrophysical characterisation of Muderong Shale: application to top seal risking: Petroleum Geoscience, v. 8, p. 371-383.

DEWHURST, D. N., YANG, Y. AND APLIN, A. C., 1999, Permeability and fluid flow in natural mudstones: In Aplin, A. C., Fleet, A. J., and Macquaker, J. H. S., (eds) Muds and Mudstones: Physical and fluid Flow Properties. Geological Society, London, Special Publications, v. 158, p. 23-43.

ENNIS-KING, J., AND PATERSON, L., 2001, Reservoir engineering issues in the geological disposal of carbon dioxide: Proceedings of the Fifth International Conference on Greenhouse Gas Control Technologies (GHGT 5), p. 290-295.

ENNIS-KING, J., AND PATERSON, L., 2003, Role of convective mixing in long-term storage of carbon dioxide in deep-saline formations: SPE Paper No. 84344: Society of Petroleum Engineers Annual Technical Conference, 12p.

FERER, M., BROMHAL, G. S., AND SMITH, D. H., 2002, Pore-level modelling of carbon dioxide sequestration in brine fields: Journal of Energy and Environmental Research, v. 2, p. 120-132.

GIBSON-POOLE, C. M., SVENDSEN, L., UNDERSCHULTZ, J., WATSON, M. N., ENNIS-KING, J., VAN RUTH, P. J., NELSON, E. J., DANIEL, R. F. AND CINAR, Y., 2006, Gippsland Basin geosequestration: Potential solution for the Latrobe Valley brown coal CO_2 emissions. The APPEA Journal, v. 46, p.413-433.

HILDENBRAND, A., SCHLOMER, S., KROOSS, B. M., AND LITTKE, R., 2004, Gas Breakthrough experiments on pelitic rocks: comparative study with N2, CO_2 and CH_4. Geofluids, v. 4, p. 91-80.

JIMENEZ, J. A., AND CHALATURNYK, R. J., 2002b, Are disused hydrocarbon reservoirs safe for geological storage of CO_2? Proceedings, 6th International Conference on Greenhouse Gas Control Technologies (GHGT 6), p. 471-476.

KIVIOR, T., KALDI, J. G., AND LANG, S. C., 2002, Seal potential in Cretaceous and late Jurassic rocks of the Vulcan Sub-Basin, North West Shelf, Australia: The APPEA Journal, v. 42, p. 203-224.

LI, S., DONG, M., LI, Z., HUANG, S., QING, H., AND NICKEL, E., 2005., Gas breakthrough pressure for hydrocarbon reservoir seal rocks: Implications for the security of long-term CO_2 storage in the Weyburn Field. Geofluids, v. 5, p. 326-334.

LINDEBERG, E., AND BERGMO, P., 2002, The long term fate of CO_2 injected into an aquifer: Sixth Conference on Greenhouse Gas Control Technologies (GHGT 6), p. 489-495.

MAZUMDER, S., PLUG, W. P., AND BRUINING, H., 2003, Capillary pressure and wettability behaviour of coal - water - carbon dioxide system: SPE No. 84339, 10p.

MORROW, N. R., CRAM, P.J., AND MCCAFFERY, F.G., 1973, Displacement studies in dolomite with wettability control by octonoic acid: AIME Petroleum Transactions, v. 255, p. 221-232.

MORROW, N.R., 1990, Wettability and its effect on oil recovery: Journal of Petroleum Technology, v. 42, p. 1476-1484.

PICKNELL, J. J., SWANSON, B. F., AND HICKMAN, W. B., 1966, Application of air-mercury capillary pressure data in the study of pore structure and fluid distribution: SPE Journal, v. 6, p. 55-61.

PURCELL, W. R., 1949, Capillary pressures - their measurement using mercury and the calculation of permeability therefrom: Petroleum Transactions - American Institute of Mining, Metallurgical and Petroleum Engineers, v. 186, p. 39-48.

ROBIN, M., 2001, Interfacial phenomena: Reservoir wettability in oil recovery: Oil & Gas Science and Technology, v. 56, p. 55-62.

ROWE, A. M. J., AND CHOU, J. C. S., 1970, Pressure-Volume-Temperature-Concentration Relation of Aqueous NaCl Solutions.: J. Chem. Eng. Data, v. 15, p. 61-66.

SAYERS, J., MARSH, C., SCOTT, A., CINAR, Y., BRADSHAW, J., HENNIG, A., BARCLAY, S., AND DANIEL, R., 2006. Assessment of a potential storage site for carbon dioxide: A case study southeast Queensland, Australia, Environmental Geosciences, v. 13, p. 123-142.

SCHOWALTER, T. T., 1979, Mechanics of secondary hydrocarbon migration and entrapment: AAPG Bulletin, v. 63, p. 723-760.

SIEMONS, N., BRUINING, H., CASTELIJNS, H., AND WOLF, K. H., 2006, Pressure dependence of the contact angle in a CO_2 - H2O - coal system: Journal of Colloid and Interface Science, v. 297, p. 755-761.

SMITH, D. A., 1966, Theoretical considerations of sealing and non-sealing faults: AAPG Bulletin, v. 50, p. 363-374.

SPAN, R., AND WAGNER, W., 1996, A New Equation of State for Carbon Dioxide Covering the Fluid Region from the Triple-Point Temperature to 1100 K at pressures up to 800 MPa: J. Phys. Chem. Ref. Data, v. 25, p. 1509-1596.

VAVRA, C. L., KALDI, J. G., AND SNEIDER R. M., 1992a, Capillary Pressure, in D. Morton-Thompson, and A.M. Woods, eds., Development Geology Reference Manual: AAPG Methods in Exploration Series, v. No. 10: Tulsa, Oklahoma, American Association of Petroleum Geologists, p. 221-225.

VAVRA, C. L., KALDI, J. G., AND SNEIDER, R. M., 1992b, Geological applications of capillary pressure: AAPG Bulletin, v. 76, p. 840-850.

WARDLAW, N. C., AND TAYLOR, R. P., 1976, Mercury capillary pressure curves and the interpretation of pore structure and capillary behaviour in reservoir rocks: Bulletin of Canadian Petroleum Geology, v. 24, p. 225-262.

WASHBURN, E. W., 1921, A note on the method of determining the distribution of pore sizes in a porous material: Proceedings of the National Academy, v. 7, p. 155-116.

YANG, D., AND GU, Y., 2004, Interfacial interactions of crude oil-brine-CO_2 systems under reservoir conditions: SPE No. 90198, 12p.

YANG, D., GU, Y., AND TONTIWACHWUTHIKUL, P., 2008, Wettability determination of the reservoir brine-reservoir rock system with dissolution of CO_2 at high pressures and elevated temperatures. Energy and Fuels, v. 22, p. 504-509

YANG, D., TONTIWACHWUTHIKUL, P., AND GU, Y., 2005, Interfacial Interactions between reservoir brine and CO_2 at high pressures and elevated temperatures: Energy and Fuels, v. 19, p. 216-223.

ZHANG, L., REN, L., AND HARTLAND, S., 1997, Detailed analysis of determination of contact angle using sphere tensiometry: Journal of Colloid and Interface Science, v. 192, p. 306-318.

ZWEIGEL, P., LINDERBERG, E., MOEN, A., AND WESSEL-BERG, D., 2004, Towards a methodology for top seal efficacy assessment for underground CO_2 storage: 7th International Conference on Greenhouse Gas Control Technologies (GHGT-7), p. 1323-11328.